Liquid Crystals
Publication details, including instructions for authors and subscription information:
http://www.informaworld.com/smpp/title~content=t713926090

Surface anchoring of nematic liquid crystal 8OCB on a DMOAP-silanated glass surface

M. Škarabot[a]; E. Osmanagič[a]; I. Muševič[a]
[a] J.Stefan Institute, 1000 Ljubljana, Slovenija

To cite this Article Škarabot, M. , Osmanagič, E. and Muševič, I.(2006) 'Surface anchoring of nematic liquid crystal 8OCB on a DMOAP-silanated glass surface', Liquid Crystals, 33: 5, 581 — 585
To link to this Article: DOI: 10.1080/02678290600617413
URL: http://dx.doi.org/10.1080/02678290600617413

Liquid Crystals, Vol. 33, No. 5, May 2006, 581–585

Surface anchoring of nematic liquid crystal 8OCB on a DMOAP-silanated glass surface

M. ŠKARABOT, E. OSMANAGIČ and I. MUŠEVIČ*
J.Stefan Institute, Jamova 39, 1000 Ljubljana, Slovenija

(*Received 19 August 2005; accepted 6 January 2006*)

Dynamic light scattering spectroscopy has been used to determine the temperature dependence of the anchoring strength of the nematic liquid crystal 8OCB on DMOAP-silanated glass surfaces inducing homeotropic alignment. Wedge-type glass cells with known thickness profile starting from 150 nm to several microns have been used in the experiments. The relaxation rates of the nematic fluctuations with the wave vector perpendicular to the confining surfaces have been measured as a function of the cell thickness. Fitting of the thickness dependence of the relaxation rate allows for straightforward determination of the surface extrapolation length and therefore also the strength of the surface anchoring, which is $1 \times 10^{-4}\,\mathrm{J\,m^{-2}}$. The overall experimental accuracy of the experiments is discussed.

1. Introduction

Anchoring of liquid crystalline molecules on confining surfaces is one of the most important issues of today's liquid crystal research [1]. A number of different experimental methods that give access to the interfacial anchoring mechanisms have been developed [1]. Among them, the dynamic light scattering technique was introduced by Wittebrood *et al.* in 1998 [2]. The method is very simple and non-invasive and relies on the measurement of the relaxation time of thermal fluctuations of the nematic liquid crystal in very thin layers with known thickness. It has been used successfully to determine the temperature dependence of the zenithal and azimuthal anchoring on polymeric orienting layers that induce planar anchoring [3].

DMOAP (*N*,*N*-dimethyl-*n*-octadecyl-3-aminopropyl-trimethoxysilyl chloride) is a very widely used surfactant that induces an excellent homeotropic alignment on glass surfaces [4]. The reason for good aligning action is that the DMOAP molecules are deposited from the solution and chemically bound to the surface. The excess material is washed away and therefore a truly monomolecular layer is formed at the surface. It has been shown in a number of second harmonic generation (SHG) optical experiments [5] and force experiments [6] that cyanobiphenyl molecules (*n*CB) form a rather complex first molecular layer that is polar (in spite of non-polar aliphatic chains of DMOAP) and tilted. This monolayer is followed by a molecular bilayer, so that in total there is a rather compact trilayer embedded into the DMOAP chains. This trilayer is responsible for the homeotropic alignment of *n*CB molecules and is stable far into the isotropic phase. So far, the surface anchoring coefficients have been determined only in the isotropic phase [7], while the strength of homeotropic anchoring in the nematic phase is unknown. This is the motivation for the present experiment.

*Corresponding author. Email: igor.musevic@ijs.si

2. Theory

The fluctuations of the nematic director in very thin cells were first treated by Stallinga *et al.* [8] and then experimentally confirmed by Wittebrood *et al.* [2]. Briefly, when the nematic liquid crystal is confined in a narrow gap between two flat surfaces, the spectrum of fluctuations is considerably altered compared with the bulk. The change is due to the anchoring of the nematic director at confining surfaces. Considering equations of motion for small fluctuations of the nematic director $\delta\mathbf{n}$ and boundary conditions at the surfaces leads to a set of dynamic equations for each degree of freedom. The general solution for the fluctuation is in a form of an overdamped orientational plane wave $\delta\mathbf{n}(\mathbf{r}, t) = \delta\mathbf{n}_0[A\cos(q_z z)+B\sin(q_z z)]\exp[\mathrm{i}(q_x x+q_y y)]\exp(-t/\tau)$ with polarization $\delta\mathbf{n}_0$. Here the z-axis is perpendicular, while the x- and y-axes are parallel to the confining walls; q_x, q_y, and q_z are the corresponding components of the wave vector $\mathbf{q}=(q_x, q_y, q_z)$ of the nematic fluctuations. There are two branches of fluctuations, i.e. the splay–bend and twist–bend branch, as described elsewhere [1]. Due to confinement, the transverse

Liquid Crystals
ISSN 0267-8292 print/ISSN 1366-5855 online © 2006 Taylor & Francis
http://www.tandf.co.uk/journals
DOI: 10.1080/02678290600617413

component of the wave vector q_z for the even modes has to fulfill the secular equation:

$$q_z \cdot tg\left(\frac{q_z d}{2}\right) = \frac{1}{L}. \quad (1)$$

Here $L=K/w$ is the surface extrapolation length, w is the surface anchoring energy, K is the corresponding effective elastic constant (in a single constant approximation), and d is the thickness of the nematic layer. In general, the secular equation (1) has to be solved numerically and has an infinite number of solutions, labelled by a discrete index $n=0, 1, 2, \ldots$, where the consecutive solutions for q_z are separated by approximately π/d. Approximate solutions of equation (1) can be obtained either for large or small extrapolation lengths. For weak anchoring and large L in comparison with d, the inverse relaxation rate of the fluctuation with a wave vector $q=(q_x, q_y, q_z)$ is

$$\tau^{-1} = \frac{K}{\gamma}\left(q_x^2 + q_y^2\right) + \frac{2w}{\gamma d} \quad (2)$$

where γ is the rotational viscosity. In the limit of strong surface anchoring, the solutions are $q_z=(n+1)\pi/d$ and the relaxation rate is

$$\tau^{-1} = \frac{K}{\gamma}\left(q_x^2 + q_y^2\right) + K(n+1)^2\frac{\pi^2}{d^2}. \quad (3)$$

For finite but still strong surface anchoring the relaxation rate for the fundamental transverse mode is

$$\tau^{-1} = \frac{K}{\gamma}\left(q_x^2 + q_y^2\right) + \frac{K}{\gamma}\frac{\pi^2}{d^2}\frac{1}{1+4L/d}. \quad (4)$$

In general the relaxation rates τ^{-1} increase with decreased thickness of the confined nematic and one can determine the surface anchoring energy density w from the fit to equations (2) or (4), depending on the anchoring regime. However, very often the approximations are not appropriate and one has to determine the anchoring energy density directly from equation (1), as will be described in this paper. Of course, the thickness of the nematic layer has to be comparable to the extrapolation length to see any departure from the strong anchoring regime, which can always be reached for sufficiently small d.

The fluctuations of the confined nematic liquid crystal can be straightforwardly observed using the dynamic light scattering technique. Here, the light scattered on orientational fluctuations is measured using photon autocorrelation technique. The particular type of fluctuations can be selected by: (i) choosing the particular direction and value of the scattering wave vector $\mathbf{k}=\mathbf{k}_i-\mathbf{k}_f$, where $\mathbf{k}_i$ and $\mathbf{k}_f$ are the wave vectors of the incident and scattered waves, respectively; (ii) varying the polarizations **i** and **f** of the incident and scattered light waves, respectively. It has been shown [8] that only those components of the fluctuations of the dielectric tensor are observable that satisfy $|q_j-(k_{fj}-k_{ij})| \leqslant \pi/B_j$, where B_j is the length of the sample in the direction $j=x, y, z$. For large dimensions, this corresponds to a delta function in the reciprocal space, and reproduces bulk condition $q_j=k_{fj}-k_{ij}$, whereas for small dimensions, it is a broadened delta function of the width π/B_j. It is also known that by selecting the appropriate polarizations of the incident and scattered waves, one observes the time-fluctuating component of the dielectric tensor for optical frequencies $\underline{\varepsilon}(\mathbf{q}, t)$ with a scattering amplitude that is equal to $\mathbf{f}\,\underline{\varepsilon}(\mathbf{q}, t)\mathbf{i}$ [1]. This allows for a selection of a given type of the eigenmode for a given wave vector.

3. Experimental

The experiments were performed on wedge-type cells made of two very flat glass slides. The surfaces of the glass had been treated by *N*,*N*-dimethyl-*n*-octadecyl-3-aminopropyltrimethoxysilyl chloride (DMOAP) as described before [7]. The cells were assembled so that a very uniform wedge was formed by the two glass slides, where one of the edges of the cell was in hard contact, while the opposite edge of the cell was separated by several micrometers. The gap in the thinnest part of the cell was of the order 100 nm, whereas the thickest part was around 1-2 μm and the length of the wedge was approximately 10 mm. This gave a change of wedge gap of the order of $200\,\mathrm{nm\,mm^{-1}}$.

The profile of the wedge was determined very accurately by two independent methods: (a) spectrophotometry on empty cells, and (b) birefringence measurements on cells filled with a liquid crystal. For spectrophotometer measurements, a very thin and elongated slit (approximately $0.25 \times 2\,\mathrm{mm^2}$) was placed in the optical path of the spectrophotometer, so that interference fringes due to the glass–air–glass gap were measured at nearly constant thickness with less than 50 nm variation. For birefringence and dynamic light scattering measurements, the cell was filled with 8OCB liquid crystal, which has the following phase sequence: isotropic–nematic transition at 80° C, nematic–smectic A transition at 67°C and smectic A–crystal transition at 54.5°C. The birefringence was measured using a photoelastic modulator-based polarimetric set-up that can measure the phase retardation between the ordinary and the extraordinary wave with an accuracy of 0.01° [1]. Both thickness profiles were then used in the same graph, as shown for a typical wedge-type cell in figure 1.

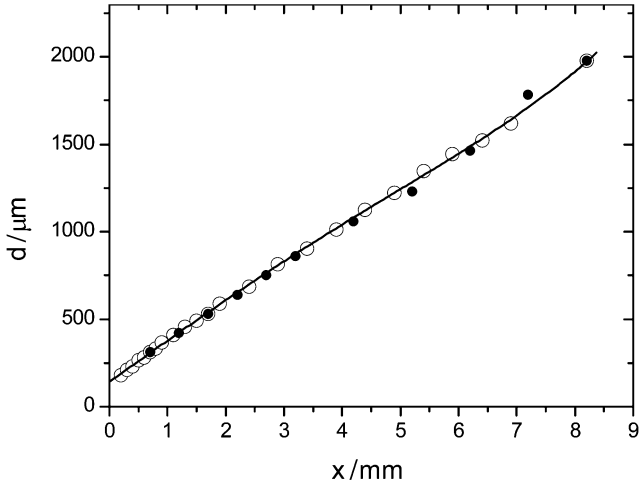

Figure 1. Thickness as a function of position of the wedge type cell. The full dots are spectrophotometric data, empty dots are birefringence data.

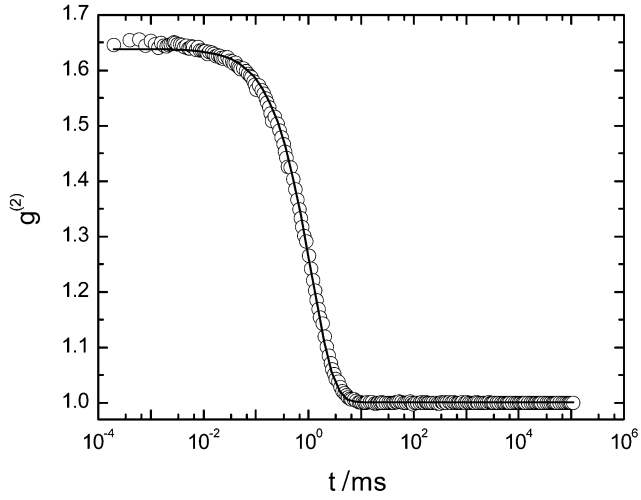

Figure 2. Typical autocorrelation function of dynamically scattered light on homeotropically oriented 8OCB in the nematic phase. The solid line represents the best single exponential fit with $\tau=(1.125\pm0.008)$ ms. The temperature is 1.5 K below T_{NI} and the thickness of the cell is 1.3 μm.

The relaxation rates of the nematic fluctuations were measured using a photon autocorrelator set-up with a logarithmic time scale. The scattering geometry was selected with the incident polarization **i** perpendicular to the nematic director $\mathbf{n}_o$ (i.e. ordinary polarization) and the depolarized scattered light was measured by setting the analyser **f** at 90° (thus detecting extraordinary scattered light). The two beams were set at directions where the scattering wave vector was $\mathbf{q}=(1.7,0,0.08)\,\mu m^{-1}$, thus lying in the plane of the cell and perpendicular to the director. In this geometry we detect nearly pure twist mode that is laterally confined by surface anchoring. A typical autocorrelation function of the scattered light on a wedge-type 8OCB cell is shown in figure 2.

4. Results and discussion

In the experiments, the relaxation rate of laterally confined twist fluctuations was measured: (i) as a function of temperature at particular thickness, and (ii) as a function of thickness at several predetermined thicknesses. Figure 3 shows the temperature dependence of the relaxation rate in the interval of the nematic phase of 8OCB.

Except for close to the I→N phase transition, the relaxation rate is nearly constant and increases in the vicinity of the N→smectic A phase transition. This is consistent with expectations, as the twist and bend elastic constants K_2 and K_3 show a pre-transitional enhancement [9] due to short range smectic order in the nematic phase, and the relaxation rate is directly proportional to these two elastic constants.

Figure 4 shows a typical thickness-dependence of the measured relaxation rates at a given temperature. The relaxation rate is shown as a function of $1/d^2$, to stress the importance of data at very small thicknesses. It is needless to say that if one wants to determine the extrapolation lengths of the order of 100 nm or less, the data at a cell thickness of several micrometers are practically irrelevant and one has to measure the most important range of thicknesses close to the expected value of the surface extrapolation length. In the

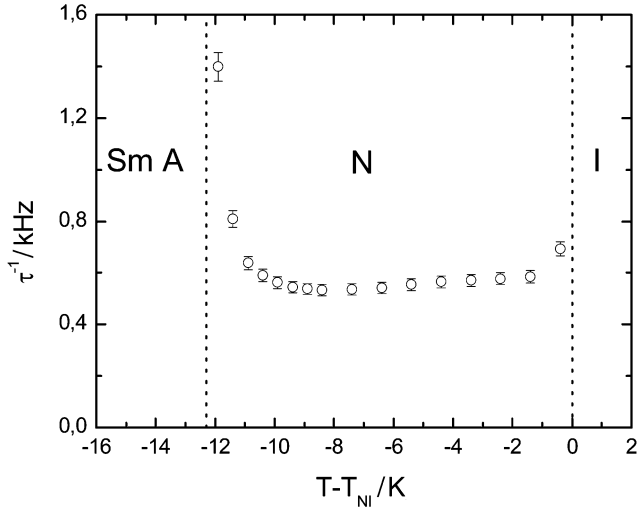

Figure 3. The temperature dependence of the fluctuation relaxation rate in the nematic phase of 8OCB. The thickness of the cell is 1.5 μm.

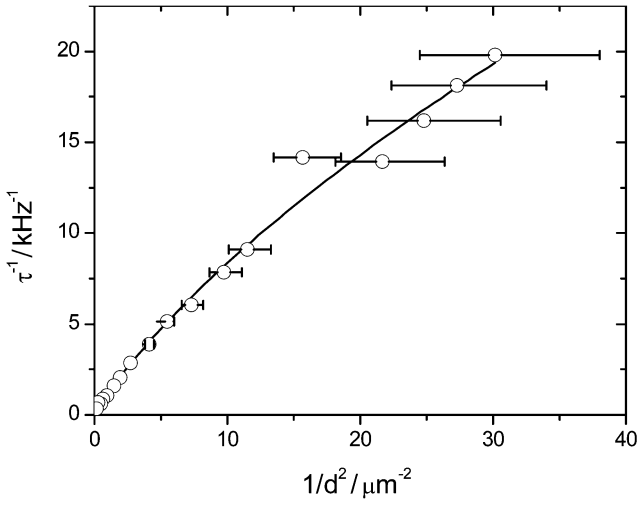

Figure 4. Typical thickness dependence of the measured relaxation rate at constant temperature 1.5 K below T_{NI}. The solid line represents the best fit to equation (4). The error bars indicate uncertainty of the actual thickness, which dominates at smaller thickness of the cell.

particular experiment shown in figure 4, the last data is collected at $1/d^2 \approx 30\,\mu m^{-2}$, corresponding to a thickness of only 180 nm.

Instead of using the approximations of Equation (4), we have determined the surface extrapolation lengths directly using the solutions of the secular equation (1). The reason for this is that the approximation (4) is valid as long as $2L << d$. In our case, $2L$ is of the order of 130 nm, which is comparable to the thickness of the cell.

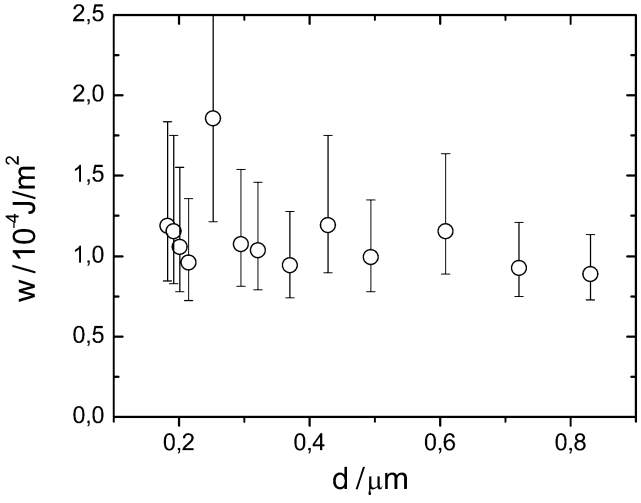

Figure 5. The surface anchoring energy, calculated as a function of the cell thickness. Each point corresponds to an individual light scattering experiment, shown in figure 4. The average value of the surface anchoring energy is calculated for each temperature.

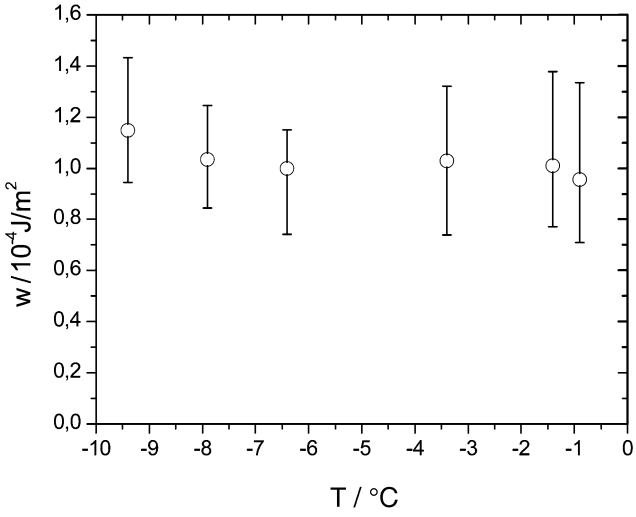

Figure 6. The temperature dependence of the surface anchoring energy for 8OCB on DMOAP-silanated glass.

The procedure of determining the surface anchoring from the measured $\tau^{-1}(d)$ was then as follows. First we determined the experimental value of τ^{-1} in the limit of large d. This is of the order of several 100 Hz and is equal to the term $K/\gamma\left(q_x^2+q_y^2\right)$ in equation (4). Second, we determined K/γ from the slope of the measured $\tau^{-1}(d)$ in the limit of large d. Third, we determined $(K/\gamma)\cdot q_z^2 = \tau^{-1}(d) - (K/\gamma)\left(q_x^2+q_y^2\right)$ from the measured relaxation rate $\tau^{-1}(d)$ for a given thickness. In combination with known K/γ this allows us to determine the transverse wave vector q_z of the fluctuation at a given thickness d. The extrapolation length L is then determined from the relation $d+2L=\pi/q_z$ and the surface anchoring energy w is determined via $L=K/w$. Here we have used data for the temperature dependence of the bend elastic constant K_3 [9]. As a result, we obtain for each measured value of the relaxation rate $\tau^{-1}(d)$ and measured local thickness the value of the surface anchoring energy. As we have measured thickness dependence of the relaxation rate, we obtain thickness dependence of the surface anchoring energy, which is fairly constant for most of our data, as shown in figure 5.

The temperature dependence of the surface anchoring energy is presented in figure 6 as a function of temperature. The anchoring energy is very large (i.e. of the order of $10^{-4}\,J\,m^{-2}$) and is nearly temperature independent, except for a very small drop of the anchoring strength that is observable close to the N→I phase transition. This can be explained within the mean field model of Faetti *et al.* [10], where the surface anchoring strength w_o is related to the surface order parameter Q_s via the relation: $Q_s^2 \approx w_o = \left[a+b(T_{NI}-T)^{1/2}\right]^2$ [10]. As w_o is practically

independent of temperature, the surface order parameter Q_s is also temperature independent, or, in another words, it is nearly saturated because of the very strong interaction with the DMOAP aligning monolayer. This means that the bulk behaviour and bulk order have little influence on the surface order parameter. Interestingly, the measured surface anchoring strength w_o is of the same order as the energy coupling coefficient that induces surface ordering in the isotropic phase of 8CB as well as 5CB [7] on DMOAP-silanated glass, as determined from atomic force microscope and ellipsometry studies. The difference between those and present experiments is, that the present experiment has been performed in the nematic phase and therefore measures the orientational coupling of the director, whereas the previous experiments were performed in the isotropic phase and measure the orientational surface coupling of the nematic order parameter.

Before concluding, let us briefly analyse the accuracy of the method we have used. The calculation of the surface anchoring energy is very sensitive to the determination of the actual sample thickness at which the relaxation rate has been measured. We estimate that the thickness is measured with an accuracy of around 25 nm. Such an error occurs if the position of the cell along the wedge direction is determined with an accuracy of 0.1 mm. Such a small systematic error of thickness in turn results in approximately 25% error of the surface anchoring energy. On the other hand, the determination of the relaxation frequency is measured with an accuracy of 2%, which contributes an additional 5% error to the determination of the surface anchoring energy. Therefore, a reasonable estimate of the overall error of the surface anchoring energy is around 30%.

References

[1] Th. Rasing, I. Muševič (Eds). *Surfaces and Interfaces of Liquid Crystals*. Springer, Berlin, Heidelberg, New York (2004).

[2] M.M. Wittebrood, Th. Rasing, S. Stallinga, I. Muševič. *Phys. Rev. Lett.*, **80**, 1232 (1998).

[3] M. Vilfan, A. Mertelj, M. Čopič. *Phys.Rev., E*, **65**, 041712 (2002); M. Vilfan and M. Čopič. *Phys.Rev. E*, **68**, 031704 (2003).

[4] F.J. Kahn, G.N. Taylor, H. Schonhorn. *Proc. IEEE*, **61**, 823 (1973).

[5] P. Guyot-Sionnest, H. Hsiung, Y.R. Shen. *Phys. Rev. Lett.*, **57**, 2963 (1986); C.S. Mullin, P. Guyot-Sionnest and Y.R. Shen. *Phys. Rev. A*, **39**, 3745 (1989); J.Y. Huang, R. Superfine, Y.R. Shen. *Phys. Rev. A*, **42**, 3660 (1990).

[6] K. Kočevar, I. Muševič. *ChemPhysChem*, **4**, 1049 (2003).

[7] K. Kočevar, I. Muševič. *Phys. Rev. E*, **64**, 051711 (2001); Kočevar, K., Muševič, I. *Phys. Rev. E*, **65**, 021703 (2002).

[8] S. Stallinga, M.M. Wittebrood, D.H. Luijendijk, Th. Rasing. *Phys. Rev. E*, **53**, 6085 (1996).

[9] J.D. Litster, J. Als-Nielsen, R.G. Birgenaeau, S.S. Dana, D. Davidov, F. Garcia-Golding, M. Kaplan, C.R. Safinya, R. Schaetzing. *J. Physique Coll. C3, Suppl. 4*, **40**, C3–339 (1979).

[10] S. Faetti, M. Gatti, V. Palleschi, T.J. Sluckin. *Phys.Rev. Lett.*, **55**, 1681 (1985).